Single-Molecule Measurement of the Strength of a Siloxane Bond†

Peter Schwaderer,‡ Enno Funk,§ Frank Achenbach,§ Johann Weis,|| Christoph Bräuchle,‡ and Jens Michaelis*,‡

Department of Chemistry and Biochemistry and Center for Nanoscience, Ludwig Maximilians Universität München, Butenandtstrasse 11, 81377 München, Germany, Wacker Chemie AG, 84489 Burghausen, Germany, and Wacker Chemie AG, Consortium Elektrochemische Industrie, 81379 München, Germany

Received August 1, 2007. In Final Form: September 19, 2007

Increasing the mechanical stability of artificial polymer materials is an important task in materials science, and for this a profound knowledge of the critical mechanoelastic properties of its constituents is vital. Here, we use AFM-based single-molecule force spectroscopy measurements to characterize the rupture of a single silicon−oxygen bond in the backbone of polydimethylsiloxane as well as the force−extension behavior of this polymer. PDMS is not only a polymer used in a large variety of products but also an important model system for highly flexible polymers. In our experiments, we probe the entire relevant force range from low forces dominated by entropy up to the rupture of the covalent Si−O bonds in the polymer backbone at high forces. The resulting rupture-force histograms are investigated with microscopic models of bond rupture under load and are compared to density functional theory calculations to characterize the free-energy landscape of the Si−O bond in the polymer backbone.

Introduction

Silicone elastomers are high-performance materials used in a wide field of applications.[1,2] Among their remarkable qualities are low-temperature dependence of the mechanoelastic properties,[3] high resistance against thermooxidation,[4] high flexibility at low temperatures,[4] adjustable release properties,[5] and physiological harmlessness.[6] However, silicone elastomers also have some disadvantages, such as relatively low ultimate mechanical strength,[7] vulnerability to hydrolytic reagents,[8] and swelling in nonpolar environment.[9] The mechanical strength of silicone elastomers is of utmost importance for many of its industrial applications, and numerous strategies exist that help to make materials capable of sustaining large deformations.[10] However, there is very little knowledge about how rupture occurs on the molecular level and the ultimate stability of the silicon-oxygen (Si−O) bond.

Single-molecule force spectroscopy has been used to study the force−extension behavior of DNA molecules,[11] proteins,[12] and polysaccharides[13] as well as the interaction of polymers with surfaces[14] or among themselves[15] and has helped to elucidate a variety of mechanical properties of polymers.[16,17] In single-molecule experiments, the exerted force can be used to rupture bonds that are extremely stable under normal conditions, with examples include the unfolding of protein domains,[18] the overstretching of DNA,[19] and the breakage of receptor−ligand linkages.[20] The high forces that can be exerted by an AFM cantilever were even used to determine the strength of covalent bonds by covalently bridging a polymer molecule between the cantilever and the glass slide surface. The experiments determined the rupture force for a particular force-loading rate.[21] Moreover, the force−extension data of many polymers can be accounted for by simple statistical physics models, such as the freely jointed chain (FJC),[22] the wormlike chain (WLC),[23] and the freely rotating chain.[24] For higher forces, these models can be expanded by the use of an enthalpic term (such as a hookian spring), yielding the extendible freely jointed chain or wormlike chain model[25] or by means of ab initio molecular dynamics calculations that describe the high force behavior prior to bond rupture.[26,27]

For a particular bond, the rupture force depends on the loading rate of the polymer.[28,29] The reason is that the dissociation rate is increased in the presence of force, an effect that can be easily understood in the Kramers theory of reaction kinetics.[30] However, when one varies the loading rate[31] or analyzes the probability

† Part of the Molecular and Surface Forces special issue.

* Corresponding author. E-mail: michaelis@lmu.de.

‡ Ludwig Maximilians Universität München.

§ Wacker Chemie AG.

|| Wacker Chemie AG, Consortium Elektrochemische Industrie.

(1) Tomanek, A. *Silicones and Industry*; Hanser: Munich, 1991; p 146.

(2) Lane, T. a. B.; Silica, S. A. Silicon and Silicones...Unraveling the Mysteries. In *Immunology of Silicones*; Potter, M., Rose, N., Eds.; Springer: Berlin, 1996.

(3) Grassie, N.; Macfarlane, I. G. *Eur. Polym. J.* **1978**, *14*, 875−884.

(4) Smith, T. L. *J. Appl. Phys.* **1964**, *35*, 27.

(5) Kricheldorf, H. *Silicon in Polymer Synthesis*; Springer: Berlin, 1996.

(6) Arkles, B. *Chemtech* **1983**, *13*, 542−555.

(7) Flaningham, O. *Chem. Anal.* **1991**, *112*, 135.

(8) Marceniec, B. a. G. J.; Urbaniak, W.; Kornetka, T. W. *Comprehensive Handbook on Hydrosilation Chemistry*; Pergamon Press: Oxford, U.K., 1992.

(9) Burkhardt, J. *Silicone Chemie und Technologie*; Vulkan Verlag: 1989.

(10) Brook, M. *Silicone in Organic Organometallic and Polymer Chemistry*; John Wiley & Sons: New York, 2000.

(11) Bustamante, C.; Bryant, Z.; Smith, S. B. *Nature* **2003**, *421*, 423−427.

(12) Fisher, T. E.; Oberhauser, A. F.; Carrion-Vazquez, M.; Marszalek, P. E.; Fernandez, J. M. *Trends Biochem. Sci.* **1999**, *24*, 379−384.

(13) Rief, M.; Oesterhelt, F.; Heymann, B.; Gaub, H. E. *Science* **1997**, *275*, 1295−1297.

(14) Hugel, T.; Seitz, M. *Macromol. Rapid Commun.* **2001**, *22*, 989−1016.

(15) Scherer, A.; Zhou, C. Q.; Michaelis, J.; Brauchle, C.; Zumbusch, A. *Macromolecules* **2005**, *38*, 9821−9825.

(16) Janshoff, A.; Neitzert, M.; Oberdorfer, Y.; Fuchs, H. *Angew. Chem., Int. Ed.* **2000**, *39*, 3213−3237.

(17) Ludwig, M.; Rief, M.; Schmidt, L.; Li, H.; Oesterhelt, F.; Gautel, M.; Gaub, H. E. *Appl. Phys. A* **1999**, *68*, 173−176.

(18) Rief, M.; Gautel, M.; Oesterhelt, F.; Fernandez, J. M.; Gaub, H. E. *Science* **1997**, *276*, 1109−1112.

(19) Smith, S. B.; Cui, Y.; Bustamante, C. *Science* **1996**, *271*, 795−799.

(20) Moy, V. T.; Florin, E. L.; Gaub, H. E. *Science* **1994**, *266*, 257−259.

(21) Grandbois, M.; Beyer, M.; Rief, M.; Clausen-Schaumann, H.; Gaub, H. E. *Science* **1999**, *283*, 1727−1730.

(22) Smith, S. B.; Finzi, L.; Bustamante, C. *Science* **1992**, *258*, 1122−1126.

(23) Marko, J. F.; Siggia, E. D. *Macromolecules* **1995**, *28*, 8759−8770.

(24) Livadaru, L.; Netz, R. R.; Kreuzer, H. J. *Macromolecules* **2003**, *36*, 3732−3744.

(25) Odijk, T. *Macromolecules* **1995**, *28*, 7016−7018.

(26) Hugel, T.; Rief, M.; Seitz, M.; Gaub, H. E.; Netz, R. R. *Phys. Rev. Lett.* **2005**, *94*.

(27) Lupton, E. M.; Nonnenberg, C.; Frank, I.; Achenbach, F.; Weis, J.; Brauchle, C. *Chem. Phys. Lett.* **2005**, *414*, 132−137.

(28) Evans, E.; Ritchie, K. *Biophys. J.* **1997**, *72*, 1541−1555.

(29) Bell, G. I. *Science* **1978**, *200*, 618−627.

(30) Evans, E. *Annu. Rev. Biophys. Biomol. Struct.* **2001**, *30*, 105−28.

10.1021/la702352x CCC: $40.75
Published on Web 11/20/2007

density function of mean rupture forces,[32−34] one can exploit this to determine the rate of reaction at zero force, the distance to the transition state, the height of the energy barrier, or the critical force at which the barrier vanishes.

For the case of polydimethylsiloxane (PDMS), the rupture of the Si−O bond has been investigated in great detail theoretically. Ab initio molecular dynamics using density functional theory (DFT) has been applied to find the rupture force as well as to determine the bond length and bond angles of Si−O oligomers stretched in vacuum,[27] in contrast to single-molecule experiments where the molecules are typically kept in a solvated environment. However, the calculations were repeated in the presence of hexamethyldisiloxane (HMDS), a typical solvent for PDMS, and it was found that the solvent has no effect on the observed rupture force.[35] In contrast, it was shown in the DFT calculations that water molecules in the vicinity of the Si−O bond can lead to lower rupture forces, an indication of a mechanically induced chemical reaction.[35]

PDMS has been studied previously using single-molecule force spectroscopy measuring the desorption forces of PDMS from mica and oxidized silicon.[36,37] Moreover, the observed force−extension behavior was analyzed using FJC or WLC models yielding a low persistence length of the polymer in air and heptane[36,37] in accordance with the idea that PDMS molecules are very flexible.

In this work, we investigate how single PDMS molecules respond to a wide variety of mechanical stresses ranging from the reduction of entropic fluctuations to the ultimate breakage of a Si−O bond in the polymer backbone. To measure the breakage of covalent bonds reliably, chemistry involving exclusively Si−O bonds was developed. The experimental results were analyzed with common force extension models to characterize the response of the silicones to force and their ability to absorb energy before rupturing. The distribution of observed rupture forces was further examined with dynamic force spectroscopy to understand the potential energy landscape of the Si−O bond. The knowledge obtained by our studies can not only improve our understanding of the properties in existing silicones but also aid the intelligent design of novel, more robust PDMS-based materials.

Materials and Methods

Sample System. In the single-molecule measurements, we used long PDMS polymers to minimize nonspecific effects between cantilever and surface. Because of the polycondensation reaction of OH-terminated PDMS oligomers, the sample is not of uniform length but contains a variety of different polymer lengths ranging from 50 to 1000 nm. To measure the rupture of the covalent Si−O bond in the PDMS backbone, it is important to attach the polymer covalently to the support surface on one side and also covalently to the AFM cantilever on the other side. A schematic of the attachment is shown in Figure 1. To facilitate the formation of a covalent bond between the PDMS and the substrate, one end of the polymer was modified by replacing all three methyl groups with chloride atoms (Supporting Information). This highly reactive system reacts spontaneously with the silanol groups of an oxidized silicon wafer (Supporting Information) to form H−Cl and a covalent Si−O bond between PDMS and the surface. On the other end of the polymer, one methyl group was replaced by a single hydrogen atom (Supporting Information). This silicon−hydrogen bond is susceptible to catalytic cleavage by a platinum-modified cantilever. The free Si bond will then covalently bind to Si−O bonds that occur frequently on the surface of a silicon nitride cantilever because of surface oxidation.[38] It is important to note that this reaction is highly specific because the presence of the platinum catalyst is required to yield measurable reaction rates. The advantage of having the platinum on the cantilever as compared to free in solution is that only PDMS molecules in close proximity to the tip of the cantilever will react whereas molecules at other locations on the silicon wafer will retain their Si−H termination. In this manner, after the covalent attachment and rupture of a PDMS bridge between the cantilever and wafer, the cantilever can simply be moved to a new location where the Si−H bond is still intact, thus allowing for fast turnover time between experiments with bicovalently attached PDMS polymers.

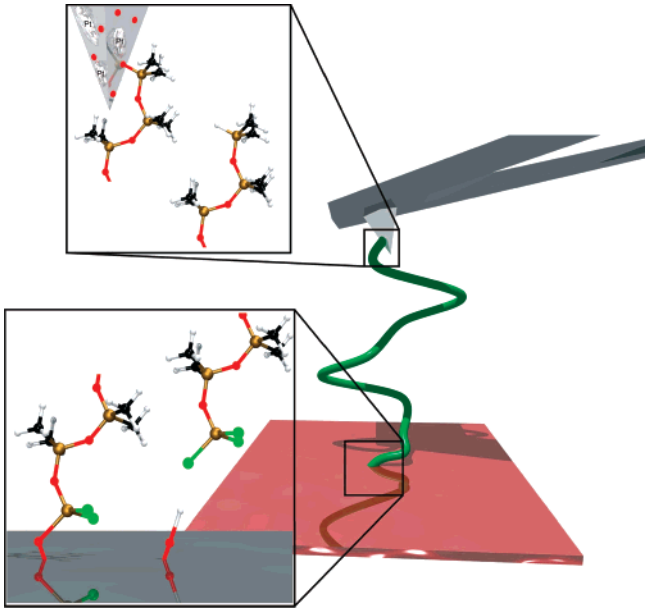

Figure 1. Schematic of the single-molecule force spectroscopy experiment showing the bicovalent attachment (not to scale). The two magnifications on the left show the two ends of the PDMS polymer, highlighting the chemical modifications in a ball-and-stick representation. Different atoms are color coded in red (oxygen), gold (silicon), green (chlorine), black (carbon), and white (hydrogen). The situations prior to (right) and after the formation of the covalent bond (left) are indicated.

Experimental Setup. All measurements were performed on a MFP3D AFM from Asylum Research with a force resolution of ∼10 pN and a sampling rate of 2 or 4 kHz. Triangular Nanoprobe Microlevers with a spring constant of ∼30 mN/m and a resonance frequency of ∼10 kHz in air were used. Each cantilever was calibrated individually by measuring its resonance frequency and inverse optical lever sensitivity in the solvent used for the single-molecule experiments (HMDS).

To attach PDMS molecules covalently to the cantilever, we used modified cantilevers that were sputtered with platinum prior to the experiment. Rather than having the whole surface of the cantilever covered with a layer of platinum, we chose sputtering conditions that allowed us to obtain a large number of isolated platinum clusters. To optimize the conditions, we used a fragment of an oxidized Si wafer exposed to the same conditions and analyzed the surface morphology of the platinum by imaging the wafer with our AFM (data not shown) as well as scanning electron microscopy (SEM) to analyze the surface morphology of the platinum clusters on the cantilever tips (Figure 2).

(31) Evans, E. *Faraday Discuss.* **1998**, *111*, 1−16.
(32) Friedsam, C.; Wehle, A. K.; Kuhner, F.; Gaub, H. E. *J. Phys.: Condens. Matter* **2003**, *15*, S1709−S1723.
(33) Dudko, O. K.; Hummer, G.; Szabo, A. *Phys. Rev. Lett.* **2006**, *96*, 108101.
(34) Dudko, O. K.; Mathe, J.; Szabo, A.; Meller, A.; Hummer, G. *Biophys. J.* **2007**, *92*, 4188−95.
(35) Lupton, E. M.; Achenbach, F.; Weis, J.; Brauchle, C.; Frank, I. *J. Phys. Chem. B* **2006**, *110*, 14557−14563.
(36) Sun, G. X.; Butt, H. J. *Macromolecules* **2004**, *37*, 6086−6089.
(37) Senden, T. J.; di Meglio, J. M.; Auroy, P. *Eur. Phys. J. B* **1998**, *3*, 211−216.
(38) Senden, T. J.; Drummond, C. J. *Colloids Surf., A* **1995**, *94*, 29−51.

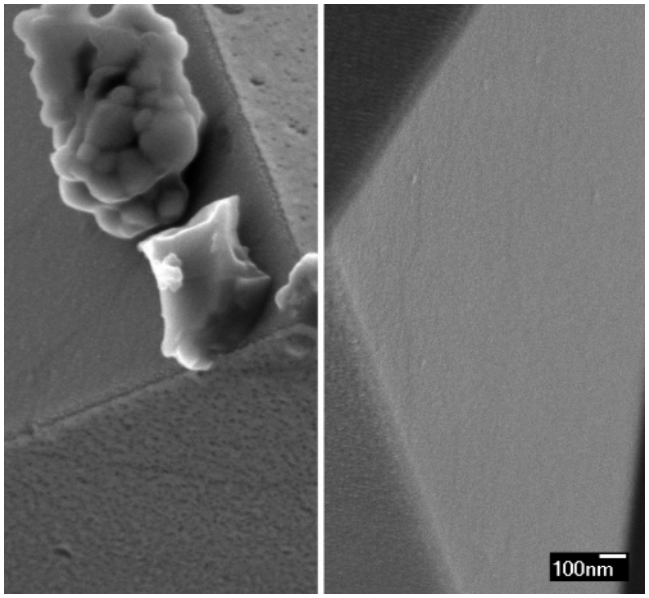

Figure 2. Platinum modification of AFM cantilever. The left image recorded with a scanning electron microscope (SEM) shows the tip of an AFM cantilever sputtered with platinum as a catalyst for the HMe_2-Si terminal end of the PDMS sample. The right SEM image shows an untreated tip for comparison.

Sample Preparation. A stock solution of PDMS (30 μL) was diluted in 4 mL of HMDS, and 30 μL of this solution was dropped onto an ~2 cm^2 piece of an oxidized silicon wafer and incubated in a nitrogen atmosphere until the solvent had evaporated. This procedure results in the covalent attachment of the PDMS molecules to the Si−O wafer through the terminal trichlorsilyl chemistry. To remove nonspecifically attached polymers, the sample was rinsed with HMDS and then washed by placing it under agitated HMDS on an orbital platform shaker for at least 2 h. Finally, the sample was rinsed again with HMDS and immediately used for single-molecule measurements.

Measurements. All experiments were performed in HMDS to maximize polymer solubility. The drawback of HMDS is its high volatility, limiting the experimental observation time to about 20 min. The high viscosity of solvents of longer silicones produced large errors in the cantilever calibration and thus prevented their utilization. Single-molecule force spectroscopy experiments were conducted by pressing the cantilever on the sample for 500 ms with a force of 5 nN to covalently attach the PDMS molecules immobilized on the surface by the platinum-catalyzed cleavage of the Si−H bond. The cantilever was then retracted with a speed of 2−4 μm/s. The force was measured by the cantilever deflection, and the extension, by a calibrated capacitive sensor, both sampled with 2 or 4 kHz. Different positions on the surface were probed by randomly changing the $x-y$ position of the sample. Measurements following this procedure showed that in ~10% of the force pulls the attached siloxane molecules typically ruptured in a single step at forces larger than 1 nN.

Scaling of Force−Extension Curves and Master Force Curves. To analyze the force−extension data of PDMS polymers, we first scaled the data from each molecule to its apparent contour length. We obtained the contour length by applying a linear fit to the high-force regime (from 1000 pN until rupture) of the polymer. According to ab initio molecular dynamics calculations performed on the rupture of PDMS oligomers by Lupton et al.,[27] the enthalpic stretching potential of the Si−O bonds is proportional to r^2; therefore, the high-force part of the extension should contribute via a linear force−distance relation. The intersection of this linear fit with the x axis (zero force) occurs at a length equal to the contour length of the molecule. For each single-molecule rupture event, the extension of the molecule is divided by the contour length, thus yielding an effective extension where a value of 1 indicates that the molecule is extended to its full contour length.

The scaled force−extension curves are then averaged to obtain a master force curve. To reduce the experimental noise, we computed the master force curve only in a force range for which we had at least 60 force−extension curves. The resulting master force curve was then again scaled to unity length using the same procedure as above. This procedure was necessary because the averaging of the individual force−extension curves had produced a small offset in length of ~0.2%.

Dynamic Force Spectroscopy Analysis. To analyze the observed probability distribution of rupture forces using dynamic force spectroscopy, one needs to know the experimental force-loading rate (k_{load}), which determines how much energy is deposited into the molecules per time. In the high-force regime (relevant for bond rupture), k_{load} can be calculated by treating the cantilever and the polymer as two Hookian springs in series. The spring constant of the cantilever is determined during the calibration of the AFM and is typically ~30 pN/nm. The spring constant of the polymer is a function of its length. However, we find that in our measurements the distribution of measured rupture forces does not change significantly with the different contour lengths present in our sample (Supporting Information). To compute k_{load}, we therefore use the mean observed polymer length ($L_C \approx 360$ nm). Moreover, we assumed that the force-loading rate in the relevant force range was linear and used the results from the linear fit to the high-force regime to determine the spring constant of the polymer. Using the spring constant of the cantilever, the spring constant of the polymer determined from our master force curve, and the experimental pulling velocity, we thus obtain a loading rate of $k_{load} \approx 34\,350$ pN/s, which we use for the dynamic force spectroscopy analysis. The dynamic force spectroscopy analysis was performed for a rupture force range of 500−2500 pN.

Experiments and Results

PDMS molecules are covalently linked to the surface of an oxidized silicon wafer and incubated with HMDS. To form a single-molecule bridge between the AFM cantilever and the wafer surface, the cantilever approaches the PDMS-covered surface and presses onto it. After a short time, the cantilever is retracted at a constant speed. With increasing distance to the surface, the force measured increases monotonically (if a molecule is attached to the cantilever) as the silicone molecule is stretched. At the maximum in the force, the weakest link in the surface−polymer−cantilever chain is broken. The data from such a single-molecule rupture experiment is shown in Figure 3 (inset). Sometimes more than one molecule is attached, resulting in a series of rupture events. Experimentally, the concentration of the PDMS molecules on the surfaces is adjusted such that more than 90% of all rupture events result in the rupture of a single cross bridge (Materials and Methods). The forces at which the molecules rupture are recorded for many single-molecule ruptures, resulting in a histogram of mean rupture forces (Figure 3). In the case of an untreated cantilever, the resulting histogram has two apparent peaks, one centered at 106 pN accounting for ~70% of all rupture events and one at ~1370 pN accounting for ~30% of all rupture events. The first peak is most likely caused by molecules that attach nonspecifically to the AFM cantilever. We can only speculate as to the nature of the second peak. One explanation could be that the extreme pressures caused by the sharp AFM tip (radius of curvature ~20 nm) being pushed onto the silicon wafer with forces of ~5 nN could cause the formation of a covalent bond. However, this process is rather uncontrolled because we do not know which bond has formed at the surface and therefore we are not sure that the experiment is solely probing the Si−O bond.

We therefore used a platinum-catalyzed reaction by sputtering the cantilever with platinum and using a Si−H-terminated polymer (Materials and Methods). Again, the AFM cantilever is pressed

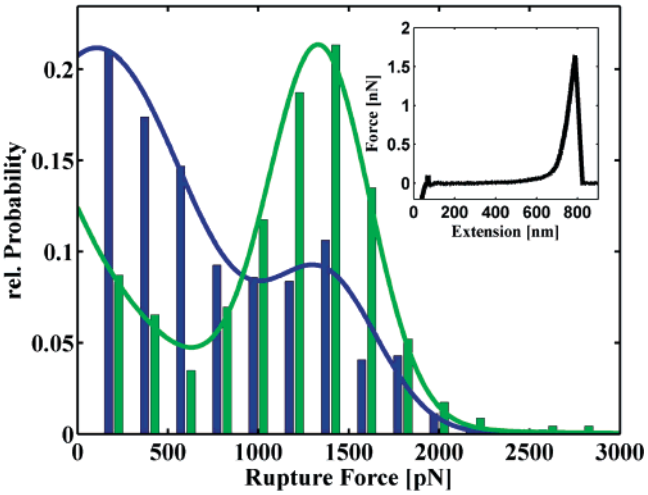

Figure 3. Histogram of rupture forces of PDMS molecules. The inset shows the data from a typical single-molecule experiment. The force at which the cross-bridge ruptures is recorded for several hundred such single-molecule force−extension curves and the results are plotted in a histogram. The histogram shows the probabilities for rupture forces in the case of an untreated cantilever (blue) computed from 450 events and a platinum-functionalized cantilever (green) computed from 250 events. The blue histogram shows that in 68% of all 450 events the rupture forces can be described by a Gaussian centered at 106 pN (σ = 184 pN). About 30% of all molecules rupture at significantly higher forces, and this behavior can be accounted for by a second Gaussian centered at around 1373 pN (σ = 103 pN). The modified cantilever results in 83% of all analyzed rupture events accumulating in a peak at around 1338 pN (σ = 98 pN).

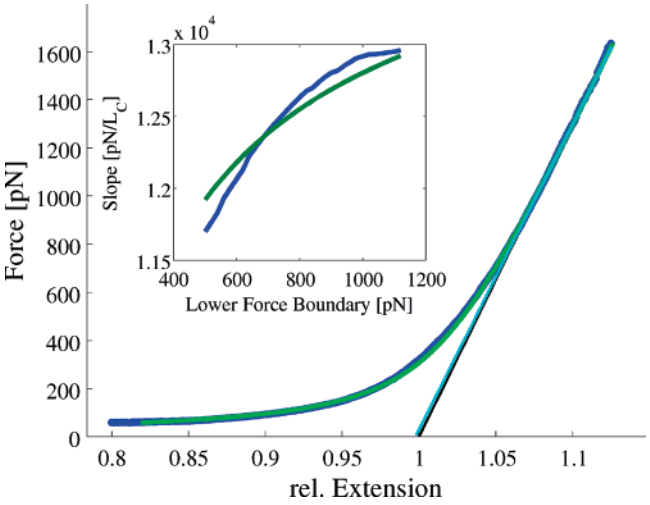

Figure 4. Force−extension curve of PDMS as described by an EFJC model. The plot shows the force−extension curve averaged from over 60 single-molecule traces with L_C > 400 nm (blue). Prior to averaging, each curve was scaled to its contour length. An EFJC fit to the data (green) nicely matches the shape of the force−extension curve and yields L_K = 0.36 nm, L_C = 1.019, and F_{char} = 14160 pN. A linear fit to the data for forces larger than 1000 pN (black line) is used for normalization. From the linear fit, one can compute the characteristic force F_{char} = 13 052 pN, which compares well to the F_{char} = 13 015 pN value obtained from a linear fit to the EFJC model in the same region (cyan). (Inset) Diagram showing the slope of the fit to the data (blue) and to the EFJC model (green) as a function of the lower force boundary.

onto the surface covered with PDMS molecules, but now the platinum on the cantilever locally catalyzes the reaction of the polymer with the cantilever tip (Figure 1). The resulting rupture force histogram is also shown in Figure 3. The histogram looks very different compared to the one obtained with unmodified cantilevers. The histogram shows a single peak centered at ∼1340 pN, which accounts for ∼85% of all observed rupture events. There are also additional rupture events that occur between 0 and 500 pN (∼15% of all observed rupture events), which are likely due to the detachment of residual noncovalently attached molecules. Thus, our experimental strategy consisting of (i) covalent attachment of the PDMS molecules to the Si−O surface of an oxidized silicon wafer, (ii) extensive washing of the wafer to remove any noncovalently attached molecules, and (iii) local covalent bond formation of the end of the PDMS molecule to the AFM cantilever catalyzed by platinum resulted in the bicovalent attachment of more than 80% of all observed rupture events. The rupture force of 1340 pN then marks the breaking of either a covalent bond in the PDMS backbone or one of the covalent bonds fixing the polymer to the substrate and to the cantilever. However, because the reaction chemistry was chosen such that we have a polymer bridge between the wafer and cantilever consisting purely of Si−O bonds, in all cases a Si−O bond is broken.

To analyze the rupture process in more detail, we now want to focus on the shape of the force−extension curves of the PDMS polymers. For low forces, the force−extension behavior is characterized by the entropic properties of PDMS as it fluctuates in the solvent. At higher forces, the stress-induced enthalpic deformation of its bond lengths and bond angles occurs. To compare the behavior of molecules of different lengths, we first need to scale the length of the molecule to its apparent contour length (Materials and Methods). The scaled force−extension curve of many single molecules is then averaged to produce the master force curve that is shown in Figure 4. This force−extension curve is fitted with a theoretical polymer-extension model to obtain the parameters describing PDMS. Because the Si−O−Si bond in the PDMS backbone is very flexible, the entropic contributions to the force−extension behavior can be approximated by assuming freely jointed chain-like behavior. Moreover, to account for the elastic deformations of the polymer, we use the elastic freely jointed chain model (EFJC), which approximates the polymer as a chain of identical springs interconnected by flexible joints. The force−extension behavior is then expressed as[39]

$$x(F) = L_C\left[\coth\left(\frac{FL_K}{k_BT}\right) - \frac{k_BT}{FL_K}\right]\left(1 + \frac{F}{F_{char}}\right) \qquad (1)$$

where F is the force, x is the extension, L_C is the contour length, and L_K is the Kuhn length.

$L_K = 2L_P$, where L_P is the persistence length, which is a measure of the polymer flexibility. F_{char} is the characteristic force of the enthalpic stretching that is related to Hookian spring constant κ of the polymer through $F_{char} = \kappa L_C$. The fit of eq 1 to our data yields L_K = 0.36 ± 0.04 nm and F_{char} = 14 200 ± 500 pN. In our analysis, we use a master force curve that has been obtained by averaging the scaled force−extension curves. Thus, we no longer have a true extension but only an extension relative to the apparent contour length. Therefore, the L_C parameter in the EFJC model is a free parameter, which, if the model fits perfectly and the scaling was performed correctly, should be unity. In fact, the best fit of the EFJC model to the master force curve yields a value of L_C = 1.019, a deviation of less than 2%, thus validating the scaling procedure. The obtained Kuhn length of L_K = 0.36 nm is fairly short, in accordance with previous publications,[37] thus validating our assumption that the molecules are very flexible.

(39) Bustamante, C.; Marko, J. F.; Siggia, E. D.; Smith, S. *Science* **1994**, *265*, 1599−600.

An extendible wormlike chain model does not describe the data as well as the EFJC model (data not shown), presumably because the short persistence length (L_P = 0.18 nm) is on the order of the length of a single bond (L_{Si-O} = 0.165 nm) and thus the coarse-grained description of the semiflexible WLC is not valid. In fact, the chain is so flexible that even for forces exceeding 1000 pN the entropic contributions are not negligible, as we will discuss now.

Ab initio molecular dynamics calculations yielded a quadratic shape of the enthalpic stretching potential of the Si−O bond,[27] thus predicting linear force−extension behavior in the limit of high load. However, even at forces above 1000 pN the force−extension data still has substantial curvature caused by the entropic nature of the polymer, an effect that is well described by the applied EFJC model. This can be seen by comparing a linear fit to the high-force regime (>1000 pN) of the master curve, which yields F_{char} and L_C for both the values obtained by the EFJC fit as well as a fit to the EFJC curve in the same force regime. The linear fit to a force−extension curve created by an EFJC fit to the data deviates only by 0.8% and 0.2% for L_C and F_{char} from the values obtained by a linear fit to the real data. In contrast, the linear fit to the data deviates from the EFJC values by 1.8 and 11% for L_C and F_{char}, respectively. We analyzed this deviation in more detail by changing the lower force at which we start the linear fit to the master force curve and find that the values asymptotically approach the values of the EFJC (Figure 4 inset). In fact, if one examines the slope of the EFJC model, one finds that only for forces above ~3800 pN can a linear fit determine L_C and F_{char} accurately (deviations smaller than 1%). Therefore, we conclude that even at forces well above 1000 pN the force−extension properties in the framework of the EFJC model are clearly influenced by the entropic contributions.

To understand the bond rupture better, it is important to determine how much energy can be deposited into PDMS material prior to material failure. Therefore, we also computed for each single molecule the total amount of energy that was deposited prior to rupture by integrating the force−extension curve. To compare the values for molecules of different lengths, we normalized the energy, yielding a histogram of energy per nanometer in length shown in Figure 5A. The histogram can be fitted by a Gaussian, yielding a mean energy/nm of 0.86 eV/nm, which can be converted to an energy per Si−O bond length of ~14 kJ/mol (L_{Si-O} = 0.165 nm). The term contains both entropic and enthalpic contributions. One can estimate the percentage of how much of the energy is actually used to deform the molecule enthalpically by again using a linear fit to the high-force regime of the force−extension curve (F > 1000 pN) and integrating the area underneath. A histogram of the relative amount of the enthalpic contribution computed in this way is shown in Figure 5B. The histogram can be fitted with a Gaussian centered at 67%. Note, however, that this analysis overestimates the enthalpic contribution because, as we have shown above, even for forces above 1 nN entropic contributions to the force−extension behavior are not negligible. If one uses the parameters obtained from the EFJC fit to the data, then the enthalpic contribution amounts to 54%. Moreover, if one compares the value of 14 kJ/mol to the binding energy of the Si−O bond of 444 kJ/mol,[40] then it becomes clear that only a small fraction of the energy is needed to rupture the covalent bond (if the energy is distributed equally along the chain). It is therefore necessary to obtain details about the potential energy landscape of the bond to understand this value. Such insight can be gained by performing dynamic force spectroscopy, which we will discuss now.

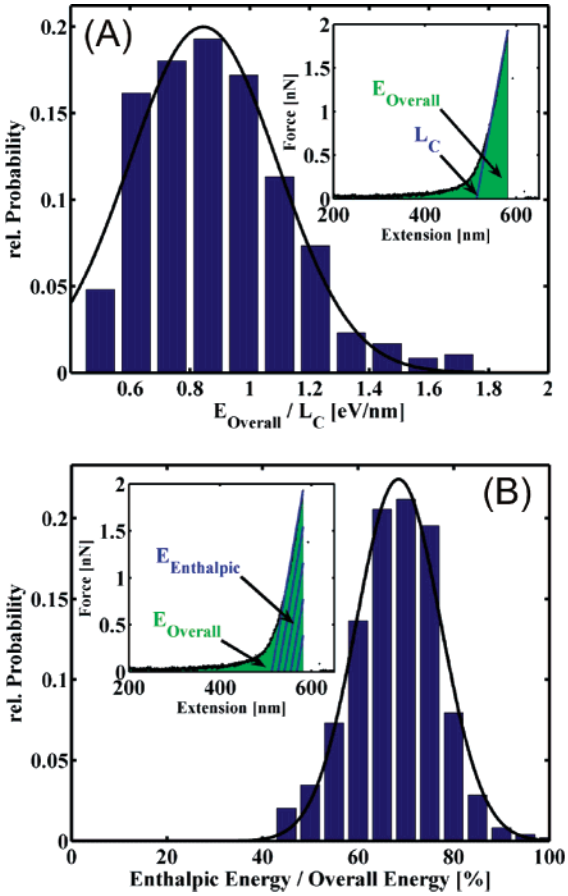

Figure 5. Histograms of energies that can be taken up by the molecules prior to rupture. (A) The histogram obtained from 1154 rupture events shows the amount of energy (in eV) per length (in nm) that is deposited in a PDMS molecule stretched in HMDS until rupture. We find that PDMS can absorb 0.86 eV/nm before breaking. (Inset) Single-molecule force−extension data, where the green area indicates the energy deposited in the polymer. (B) Histogram showing the relative amount of enthalpic deformation with respect to the total amount of energy that the molecule can take up prior to rupture. The value for the enthalpic energy is computed by integrating the area underneath a linear fit to the data above 1000 pN, as illustrated in the inset (striped area).

Dynamic force spectroscopy (DFS) is used to gain insight into the kinetic rupture properties of the Si−O bond in the PDMS backbone. In DFS, one commonly assumes that the breaking of a bond corresponds to the diffusion of the initial state, bound in a single well in the energy landscape, across an activation barrier of height $\Delta G^{\ddagger}$ at a distance $x^{\ddagger}$ along the reaction coordinate. (See Figure 6 for an illustration.) Applying a force tilts the energy landscape and thus increases the escape probability. Using Kramers' rate theory,[41] one can describe the rupture of the bound to the dissociated state in the presence of an external force. In this model, one can obtain characteristic parameters for the investigated system. Several different approaches to analyze the measured data are currently used in the literature. The earlier phenomenological models[30] assume a small reduction of the barrier by the applied force without changing the distance between the energy minimum and the transition state. However, as the force increases, the distance between the energy minimum and the transition state decreases. Using Kramers' theory of diffusive barrier crossing under an applied force, alternative models have recently been developed.[42,43] With these models, one can extract the intrinsic dissociation rate at zero force, k_0, the height of the

(40) Hollemann, A. F.; Wiberg, N. *Inorg. Chem*. Academic Press: 2001.

(41) Kramers, H. A. *Physica* **1940**, *7*, 284−304.

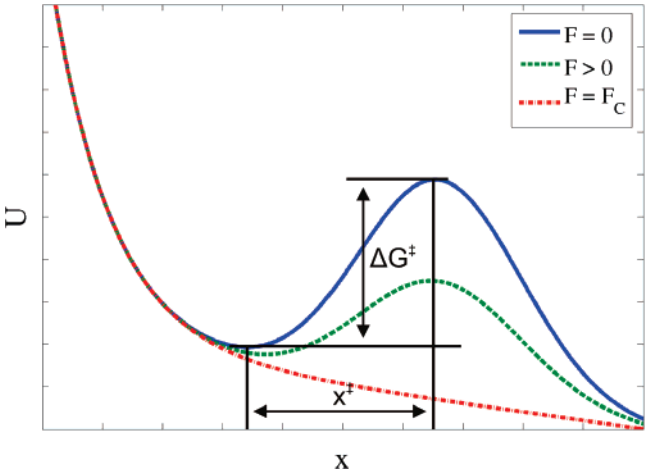

Figure 6. Force dependence of the energy landscape. The graph schematically shows the dependence of the Si−O bond's potential energy landscape as a function of force. Note that the pulling direction directly defines a reaction coordinate x, along which the distance to the transition state, $x^{\ddagger}$, is measured. The transition state has a Gibbs free energy that is higher than the Gibbs free energy of the bound state by $\Delta G^{\ddagger}$. Force tilts the potential energy surface until at a critical force of F_C the barrier vanishes completely.

potential barrier, $\Delta G^{\ddagger}$, and the distance to the transition state, $x^{\ddagger}$, from the probability distribution of rupture forces[33]

$$p(F) = \frac{1}{k_{\text{load}}} k(F) e^{k_B T k_0 / x^{\ddagger} k_{\text{load}}} e^{-k(F) k_B T / x^{\ddagger} k_{\text{load}} ((1 - \nu F x^{\ddagger}/\Delta G^{\ddagger})^{1 - (1/\nu)}} \tag{2}$$

where k_{load} is the force-loading rate and the force-dependent rate of bond rupture, $k(F)$, is shown to have the following form:[33]

$$k(F) = k_0 \left(1 - \frac{\nu F x^{\ddagger}}{\Delta G^{\ddagger}}\right)^{1/(\nu - 1)} \exp\left\{\frac{\Delta G^{\ddagger}}{k_B T}\left[1 - \left(1 - \frac{\nu F x^{\ddagger}}{\Delta G^{\ddagger}}\right)_{1/\nu}\right]\right\} \tag{3}$$

From the determined values for $\Delta G^{\ddagger}$ and $x^{\ddagger}$, one can compute the critical force at which the barrier vanishes completely, F_{crit}, by

$$F_{\text{crit}} = \frac{\Delta G^{\ddagger}}{\nu x^{\ddagger}} \tag{4}$$

Different free-energy surfaces are distinguished in the equations by different values for ν.

(i) $\nu = {}^1/_2$ applies to a cusp model, where $U_0(x) = \Delta G^{\ddagger}(x/x^{\ddagger})^2$ for $x < x^{\ddagger}$ and $U_0(x) = -\infty$ elsewhere.

(ii) $\nu = {}^2/_3$ for the linear-cubic model, where $U_0(x) = ({}^3/_2)\Delta G^{\ddagger}(x/x^{\ddagger}) - 2\Delta G^{\ddagger}(x/x^{\ddagger})^3$.

(iii) For $\nu = 1$ (or $\Delta G^{\ddagger} = \infty$), eqs 2 and 3 reduce to those of the earlier phenomenological model.

We tried to fit both microscopic models as well as the phenomenological model to our measured data (Figure 7). Although the observed probability distribution can be qualitatively obtained by all three approaches, it is obvious that the fits to the two microscopic models follow the observed data better than that to the phenomenological model. Moreover, in the high-force regime, the distribution obtained by fitting to the cusp potential can reproduce the observed shape better than the linear-cubic potential, making it our preferred model. From the fit to the data using the cusp potential, we obtain $k_0 = 0.52\ s^{-1}$, $\Delta G^{\ddagger} = 30.4$ pN nm, and $x^{\ddagger} = 0.021$ nm. With these values, we can also compute $F_{\text{crit}} = 2900$ pN.

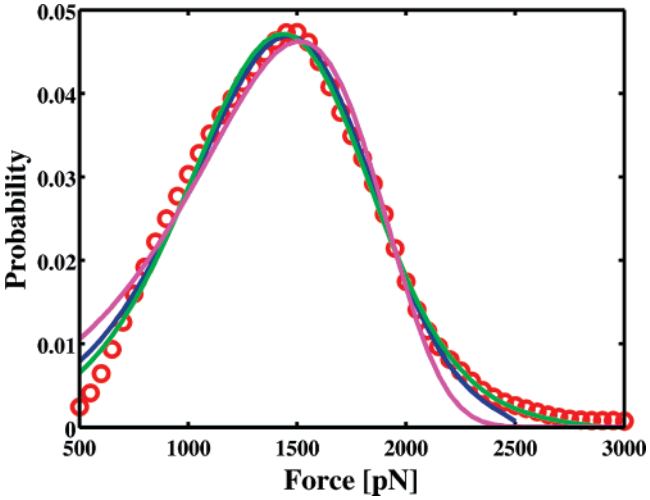

Figure 7. Probability density distribution of rupture forces. Measured probability distribution of rupture forces $P(F)$ of 1154 rupture events (red circles) recorded at a force loading rate of $k_{\text{load}} \approx 34\,350$ pN/s (Materials and Methods) and theoretical models. Blue line: the fit to eq 4 using $\nu = {}^2/_3$ (linear-cubic potential) yields $k_0 = 0.97\ s^{-1}$, $\Delta G^{\ddagger} = 26.5$ pN nm, $F_{\text{crit}} = 2484$ pN, and $x^{\ddagger} = 0.016$ nm. Green line: the fit to eq 2 using $\nu = {}^1/_2$ (cusp potential) yields $k_0 = 0.52\ s^{-1}$, $\Delta G^{\ddagger} = 30.4$ pN nm, and $x^{\ddagger} = 0.021$ nm, thus using eq 4, we obtain $F_{\text{crit}} = 2895$ pN. Magenta line: the fit to the phenomenological model yields $k_0 = 2.3\ s^{-1}$ and $x^{\ddagger} = 0.010$ nm. Although all three models describe the data reasonably well, it is clear that the cusp potential (green line) can best reproduce the observed shape of the probability density function.

The microscopic model was developed for the rupture of a single bond. In our case, we have a polymer formed from many covalent bonds in series. Therefore, to obtain the rate for the rupture of a single covalent bond, $k_0^{\text{singlebond}}$, we have to divide the observed k_0 by N, the number of covalent bonds in the polymer. From our observed mean contour length of $L_C \approx 360$ nm, we estimate $N \approx 2200$ and thus a rate constant of $k_0^{\text{singlebond}} \approx 2.4 \times 10^{-4}\ s^{-1}$.

Caution must be taken when looking at the values obtained by fitting the microscopic model to our data. The height of the energy barrier and the distance to the barrier match our expectations and compare well to the values obtained from DFT calculations (see below). In contrast, the rate at zero load is much too high and does not match our common knowledge that a covalent Si−O bond in the absence of mechanical stress is extremely stable. It is clear that in this respect the model fails to give an accurate picture, an effect that has been noted previously.[33] We can only speculate as to why in our experiment the determination of k_0 was so unsuccessful: (i) There is probably still a small percentage of noncovalent bonds within our histogram that might skew the results. (ii) For $F_{\text{rupture}} \approx F_{\text{crit}}$ forces, the model is not correct because the theory was developed in the limit of a high energy barrier.[33] (iii) There might be additional effects that occur only at high loads (e.g., hydrolytic attacks by a small contamination of water in our solvent[35]). (iv) The forces required to rupture the covalent bond on an experimentally relevant time scale are fairly high, and thus the extrapolation to zero load is likely to be inaccurate, resulting in a rupture rate that is higher than what is expected and therefore also in a barrier that is too low.

For a better understanding of the rupture process, it is helpful to compare the experimentally observed values for the breaking

(42) Dudko, O. K.; Filippov, A. E.; Klafter, J.; Urbakh, M. *Proc. Natl. Acad. Sci. U.S.A.* **2003**, *100*, 11378−11381.
(43) Hummer, G.; Szabo, A. *Biophys. J.* **2003**, *85*, 5−15.

of the Si−O bond to predictions that have been made for the rupture of a PDMS oligomer based on Car−Parrinello molecular dynamics (CPMD) using DFT to describe the electrons.[27] In these calculations, the observed bond length at rupture was 1.8−1.9 Å (compared to 1.65 Å in the relaxed state), in good agreement with the distance to the transition state observed in our dynamic force spectroscopy analysis ($x^{\ddagger} = 0.21$ Å). Moreover, in these calculations the rupture force for a pulling speed of 55 m/s changed from 6.6 nN for a dimer to 5.2 nN for a trimer to 4.6 nN for a hexamer to 4.4 nN for a decamer.[27] Thus, the mechanical energy that is put into the system can redistribute over several bonds, lowering the threshold for rupture as the length of the PDMS molecule is increased. To compare these values with those obtained by our single-molecule rupture events, one should note that the polymer length used in the single-molecule experiments was several orders of magnitude longer than in the CPMD calculations ($N \approx 2200$ compared to $N = 2-10$). Moreover, the pulling velocities differed by 7 orders of magnitude (2 μm/s vs 55 m/s), and edge effects are of much higher importance for the short oligomers used in the theoretical studies. Thus, the difference between the mean rupture force of ∼1.3 nN observed experimentally and ∼4.4 nN predicted theoretically can be understood. However, one might ask why, in the single-molecule experiments even though molecules of $N \approx 300-6000$ were used, no systematic dependence of the observed rupture force on length was observed. This can be explained by an effective length over which the mechanical energy can redistribute and the fact that this effective length is much smaller than the polymer lengths investigated. Our data even allow us to make a rough estimate of this effective length by comparing the energy of the Si−O bond (444 kJ/mol) to the energy that is needed to rupture the polymer. If one integrates the force−extension curve of our PDMS polymers (approximated bf the EFJC fit) from 0 pN to $F_{crit} \approx$ 2900 pN, then one obtains $E^{exp}_{Si-O} \approx 35$ kJ/mol. Therefore, the effective number of bonds over which the energy is free to redistribute is given by $n \approx 443$ kJ mol^{-1}/35 kJ mol$^{-1} \approx 15$.

Conclusions

Our AFM experiments give insight into the mechano-elastic properties of single PDMS molecules under critical tensile stress. We find that PDMS solvated in HMDS shows force−extension behavior that is well described by an elastic freely jointed chain model with a persistence length of $L_P = 0.18$ nm and a characteristic force of $F_{char} = 14\,200$ pN. On average, we could deposit 0.86 eV energy per nm polymer length (or 14 kJ/mol) in the molecules prior to breaking the covalent attachment. Part of this energy (54%), was used in the enthalpic deformation of the molecules. However, these values are only a small percentage of the energy of the Si−O bond (444 kJ/mol). In a PDMS polymer, the mechanical energy that is deposited into the molecule can redistribute, thus lowering the observed barrier of bond rupture in accordance with theoretical predictions. The probability distribution of rupture forces was analyzed with different force spectroscopic methods to extract the microscopic parameters relevant to the breaking of the Si−O bond in the siloxane backbone. We determine the critical force at which the barrier between the bound and the unbound state vanishes, $F_{crit} = 2900$ pN, the barrier height of $\Delta G^{\ddagger} = 30.4$ pN nm, and a distance of $x^{\ddagger} = 0.021$ nm to the minimum of the potential well. For $F = 0$ pN, we infer a dissociation rate of $k_0^{singlebond} \approx 2.4 \times 10^{-4}$ s^{-1}. The rate of dissociation at zero force is several orders of magnitude higher than what is expected. Possible explanations include the influence of statistical energy fluctuations due to the entropy of long polymers, the presence of water in the solvent, edge effects at the terminal bonds to the cantilever or the substrate, or the presence of noncovalently bound molecules in the evaluated data set. The high forces needed to rupture covalent bonds on a reasonable time scale, however, might make the extrapolation to zero load fairly inaccurate. Therefore, new theoretical models need to be developed to infer characteristic parameters at zero load from high-force measurements. Another experimentally feasible approach would be to measure the time that the polymer can sustain a certain force by implementing a force feedback mechanism in the experimental apparatus. These experiments will be the subject of future studies.

Acknowledgment. We thank Irmgard Frank for helpful discussions, Stefan Schöffberger for the platinum sputtering of the cantilevers, Steffen Schmidt for the scanning electron microscopy of the modified cantilevers, and Chunqing Zhou and Armin Fehn for their contributions in the early stages of the experiments. This work was supported by the Deutsche Forschungsgemeinschaft (Sonderforschungsbereich 486) and by the Nanosystems Initiative Munich.

Supporting Information Available: Details of the oxidation of the silicon wafer, the synthesis of the siloxane polymer, and the rupture force as a function of polymer length. This material is available free of charge via the Internet at http://pubs.acs.org.

LA702352X